CHARACTERIZATION OF PHASE CHEMISTRY IN SOL-GEL NaSICON

Erik D. Spoerke,[1,*] Bonnie B. McKenzie,[2] Nelson S. Bell,[1] Cynthia Edney,[1] Jill S. Wheeler,[1] and David Ingersoll[3]

[1] Electronic, Optical, and Nano Materials, Sandia National Laboratories, Albuquerque, NM USA 87123
[2] Materials Characterization and Performance, Sandia National Laboratories, Albuquerque, NM USA 87123
[3] Power Sources Research and Development, Sandia National Laboratories, Albuquerque, NM USA 87123

*Corresponding author:
Erik D. Spoerke, Ph.D.
Electronic, Optical, and Nano Materials
Sandia National Laboratories
PO Box 5800 MS 1411
Albuquerque, NM USA 87185
edspoer@sandia.gov

ABSTRACT

NaSICON ceramics are promising solid-state electrolytes for sodium-based battery development, but the performance of these materials can be dramatically affected by the presence of secondary, contaminant phases. Characterization of these phases by traditional x-ray diffraction and scanning electron microscopy, however, can provide an incomplete picture of the secondary phase integration with a NaSICON ceramic. Here, we describe how the utilization of backscattered electron imaging and energy-dispersive x-ray spectroscopy can be used to provide a more complete analysis of secondary phase morphology, distribution, and composition in these materials. Insights from this more comprehensive characterization approach are expected to provide a better understanding of the influences of secondary phases on NaSICON performance and inform the development of improved solid-state electrolytes for new sodium-based battery technologies.

Keywords: *NaSICON, phase chemistry, energy dispersive x-ray spectroscopy, backscattered electron microscopy*

INTRODUCTION

Realizing the potential of emerging sodium ion chemistries depends on the development of a robust, efficient solid-state electrolyte with high ionic conductivity that is also capable of physically separating molten sodium and incompatible catholytes. The sodium ion conducting ceramic NaSICON ($Na_{1+x}Zr_2P_{3-x}Si_xO_{12}$, $0 \leq x \leq 3$) has shown promise as a capable solid state electrolyte with excellent sodium ion conductivity,[1-5] but it is prone to the formation of deleterious secondary phases such as ZrO_2, sodium silicates, sodium phosphates, and amorphous, glassy materials, particularly when formed at high temperatures (>1200°C).[6-8]

Depending on the quantity, distribution, and composition of these contaminant phases, their presence can significantly degrade the performance of the NaSICON ceramic materials. Zirconia and various silicate phases are believed to decrease ionic conductivity, while phosphates and glassy phases are believed to be chemically unstable against a variety of electrolytes, leading to potential concerns over ceramic integrity and reliability.[6, 8-13] This latter issue is particularly important when the NaSICON is required to physically separate, for example, molten sodium from potentially violently reactive electrolytes. Naturally, characterizing the composition and distribution of these secondary phases is central to understanding their influences on NaSICON performance and ameliorating any deleterious affects associated with these contaminant phases.

Too often, however, literature reports of these materials rely almost exclusively on x-ray diffraction (XRD) or scanning electron micrographs obtained using traditional secondary electron imaging to characterize the phase chemistry of the synthesized materials.[1, 5, 14-19] Certainly, XRD remains a time-tested, indispensible analytical technique that can provide important information about the presence, crystal structure, and even composition of crystalline ceramic phases. Unfortunately, the detection of amorphous glassy phases or the determination of phase distribution in a sample can be difficult or impossible to achieve with diffraction alone. Similarly, commonly used secondary electron imaging in an SEM provides valuable information about particle size and topography in ceramic materials, but it can be difficult to identify chemically distinct phases using this approach. Here, utilizing a sol-gel preparation of NaSICON as a model system, we demonstrate how relatively standard techniques such as scanning electron imaging with backscattered electrons and careful application of energy dispersive x-ray analysis can provide a much more comprehensive picture of the secondary phase chemistry in these potentially important sodium ion-conducting materials.

METHODS AND MATERIALS

Synthesis of NaSICON ceramic powders was adapted from the procedure reported by Porkodi *et al*.[20] Zirconium (IV) butoxide (80 wt% in 1-butanol, Sigma-Aldrich) was mixed in a 1:2 molar ratio with acetylacetone (acac, Sigma-Aldrich, Reagent Plus, >99%) in 2-propanol solution (Sigma-Aldrich, anhydrous) under magnetic stirring. The Zr-acac solutions were yellow and transparent. The Zr source was gravimetrically assayed for accurate Zr-content.

For the $Na_3Zr_2PSi_2O_{12}$ composition, $Na_3PO_4 \cdot 12H_2O$ was dissolved in deionized water (0.4M in 500mL) and the pH was adjusted to 11.8 using concentrated HNO_3. A stoichiometric quantity of tetraethylorthosilicate (TEOS) (Aldrich, >99%) was added to the reaction vessel, forming a phase separated liquid. Rapid stirring mixed the phases until the TEOS reacted to form an opaque white precipitate. The stoichiometric amount of Zr-acac solution in 2-propanol was added rapidly and precipitated a white gel. The precipitate was aged for 2 h and collected by rotary evaporation. Full dryness was obtained under vacuum at 75°C for 3 days.

For the $Na_4Zr_2Si_3O_{12}$ composition, stoichiometric quantities of TEOS and Zr-acac were mixed in isopropanol solvent to create a transparent, yellow solution. 50 ml of deionized water was used to dissolve sodium hydroxide under stirring for 2 hours. The aqueous solution of NaOH was added rapidly to the isopropanol solution and stirred vigorously for 10 minutes. The solution remained transparent. The contents were dried and recovered by rotary evaporation, with final drying of the product under vacuum at 80°C for 1 day.

Dry NaSICON precursor powders were manually crushed with mortar and pestle before calcining in flowing air (4.7 l/min) at 800°C for 12 hours. Binder (1% polyvinyl alcohol/polyethylene glycol, added as aqueous solution) was added and the pellets were dried at 60°C overnight. Pellets were formed by isostatic pressing at 10 ksi in a cylindrical steel die. Sintering was performed in air at 1000°C for 12 hours.

Scanning electron microscopy was performed using a Supra 55VP field emission gun scanning electron microscope at an accelerating voltage of 15kV. Energy dispersive x-ray analysis was performed using a Bruker quad SDD detector and Esprit software. Energy dispersive x-ray analysis used to differentiate Zr and P was performed at 25kV.

RESULTS AND DISCUSSION

Figure 1 shows a series of scanning electron micrographs taken from NaSICON pellets. The images in the left column (a,c,e,g) were taken using standard secondary electron (SE) imaging. The images in the right column (b,d,f,h) were taken of the exact same field of view, but were imaged using backscattered electrons (BSE). The nature of each of these imaging approaches allows each to provide different information about a

sample. In secondary electron imaging, the image is produced from relatively low energy electrons emitted during the inelastic scattering of the high energy incident electrons. These secondary electrons are generated both at the sample's surface and from within an electron interaction volume extending tens to hundreds of nanometers into the sample (though depth depends on incident electron energy). These secondary electrons, then, provide potentially high resolution imaging of surface topography and sample morphology. In contrast, backscattered electrons are high energy electrons that have been elastically scattered off the sample surface. Although these electrons typically provide little or no information about sample morphology, the elastic scattering is sensitive to the atomic number (Z) of the scattering atom. Generally, higher Z produces more efficient elastic scattering, and higher detectable signal. As a result, the contrast in backscattered images is affected by the chemical composition of a sample.

These effects are evident in Figure 1. The SE images on the left clearly show the complex morphological details of the samples, while the BSE images on the right, while relatively "flat" in appearance clearly highlight differences in material phase as a function of differences in composition. Comparing Figures 1a and 1b, small crystals of a secondary phase with a higher average Z, (determined to be ZrO_2) appear much more clearly as bright white particles against the relatively darker NaSICON background. Although XRD may be able to identify that zirconia is present as a secondary crystalline phase in the NaSICON ceramic, these BSE images provide critical insights into the distribution of these zirconia particles, answering questions about whether or not the ZrO_2 formed as a continuous phase, as discrete particles, or if the particles are localized, for example, along grain boundaries. This information can be critical in determining if the ZrO_2 will significantly impact ion conduction. Similar comparisons are presented in figures 1c-h. Comparing figure 1c and 1d, the BSE image in Figure 1d clearly reveals the presence of secondary phases in $Na_4Zr_2Si_3O_{12}$ difficult or impossible to detect in the SE image of Figure 1c. The relatively darker contrast of the contaminant phases is consistent with the ultimate identification of these phases as silicate inclusions (see below). Figures 1e and 1f show the presence of glassy inclusions in $Na_3Zr_2PSi_2O_{12}$ that are not readily detected by XRD. Although these inclusions are morphologically distinct enough to be visible using SE imaging, the glassy components (dark inclusions in Figure 1f), are much more readily visible in the BSE image. Finally, Figures 1g and 1h show a structurally and chemically complex image. Although it is clear from the SE image in Figure 1g that there are secondary phase inclusions present, the brightly highlighted particles in the BSE image in Figure 1h much more clearly reveal the extent of the secondary phase contamination and provide key insights into how this contaminant is distributed within the ceramic.

Certainly, these examples illustrate the potential value of using BSE imaging to characterize the phase chemistry of NaSICON ceramics. The addition of energy dispersive x-ray spectroscopy (EDXS), however, provides even more key information about these secondary phases. EDXS utilizes x-rays emitted from atoms excited during the inelastic scattering of incident electrons. The energy of the emitted x-rays is directly tied to the different electron shells of the excited atoms. Because these energy levels are unique to each atomic element, the distribution of emitted x-ray energies can provide very specific information about the chemical composition of a sample. As shown in Figure 2, this extremely useful technique can be applied to the characterization of the secondary phases highlighted using the BES images in Figure 1. Figure 2a, Figure 2b, and Figure 2c are each composed for four component images: a BSE image (black and white) of a NaSICON sample, elemental maps indicating the presence of Si, Zr, and Na in the corresponding images. Oxygen (not shown) was found to correlate with all of these components. Figure 2a, taken from a sample of $Na_3Zr_2PSi_2O_{12}$, shows a strong correlation between the bright white contaminants (like those in Figure 1b) and zirconium with a negative correlation to silicon or sodium, indicating that these particles are likely zirconium oxide. Figure 2b identifies the composition of secondary phases such as those seen in Figure 1d. There is a strong correlation between dark inclusion in the BSE image and both sodium and silicon. Together with the negative correlation to zirconium, these images suggest this phase is a sodium silicate phase in $Na_4Zr_2Si_3O_{12}$. Figure 2c characterizes the composition of glassy inclusions from $Na_3Zr_2PSi_2O_{12}$, similar to those seen in Figure 1f. A high correlation with silicon, with a limited or absent correlation to sodium and zirconium suggests these glassy components are silica glasses, possibly containing small amounts of sodium.

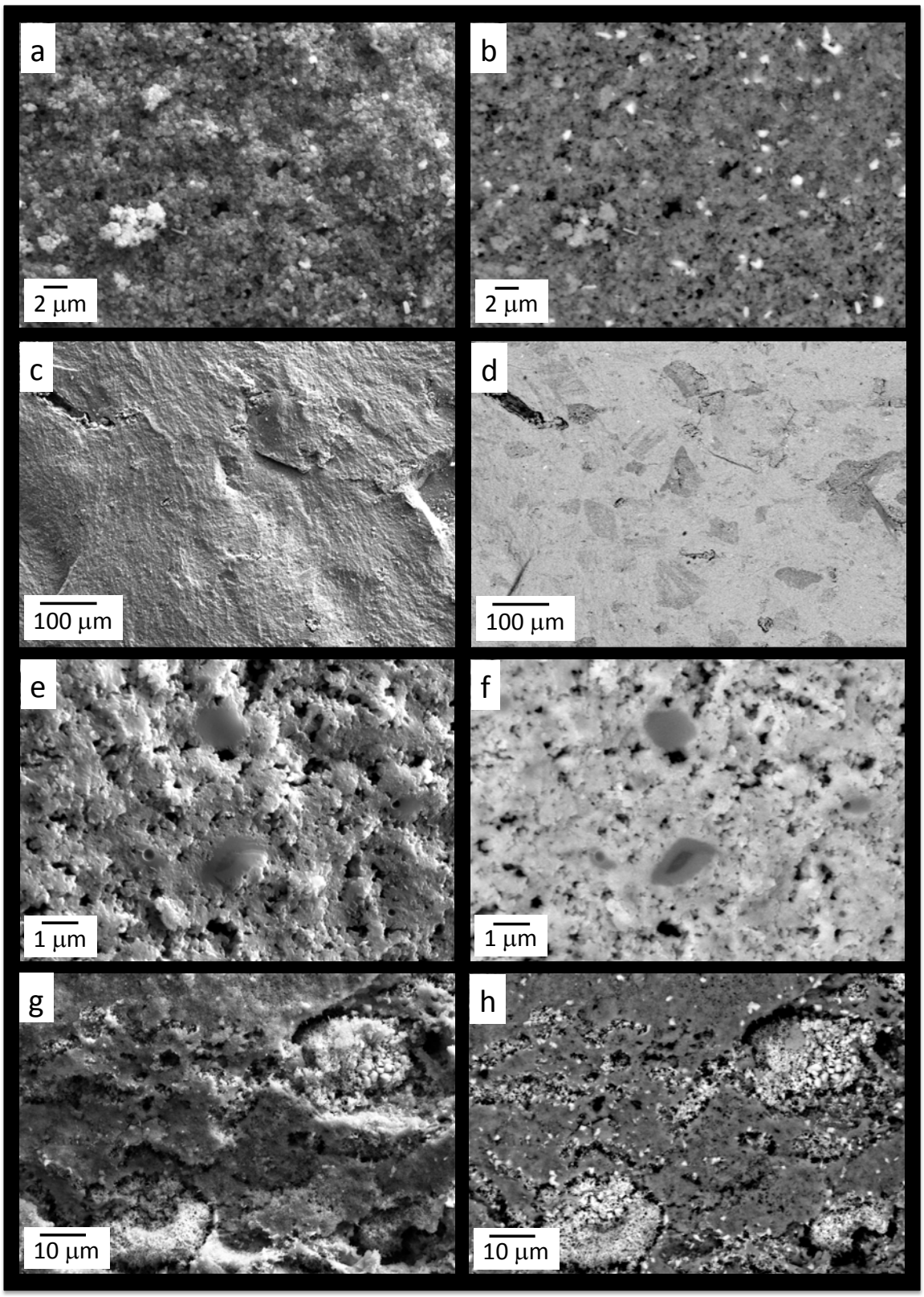

Figure 1. *Scanning electron microscope images collected using secondary electron imaging (a,c,e,g) and backscattered electron imaging (b,d,f,h). Images in the left column were taken from the same field of view as the corresponding images in the right column.*

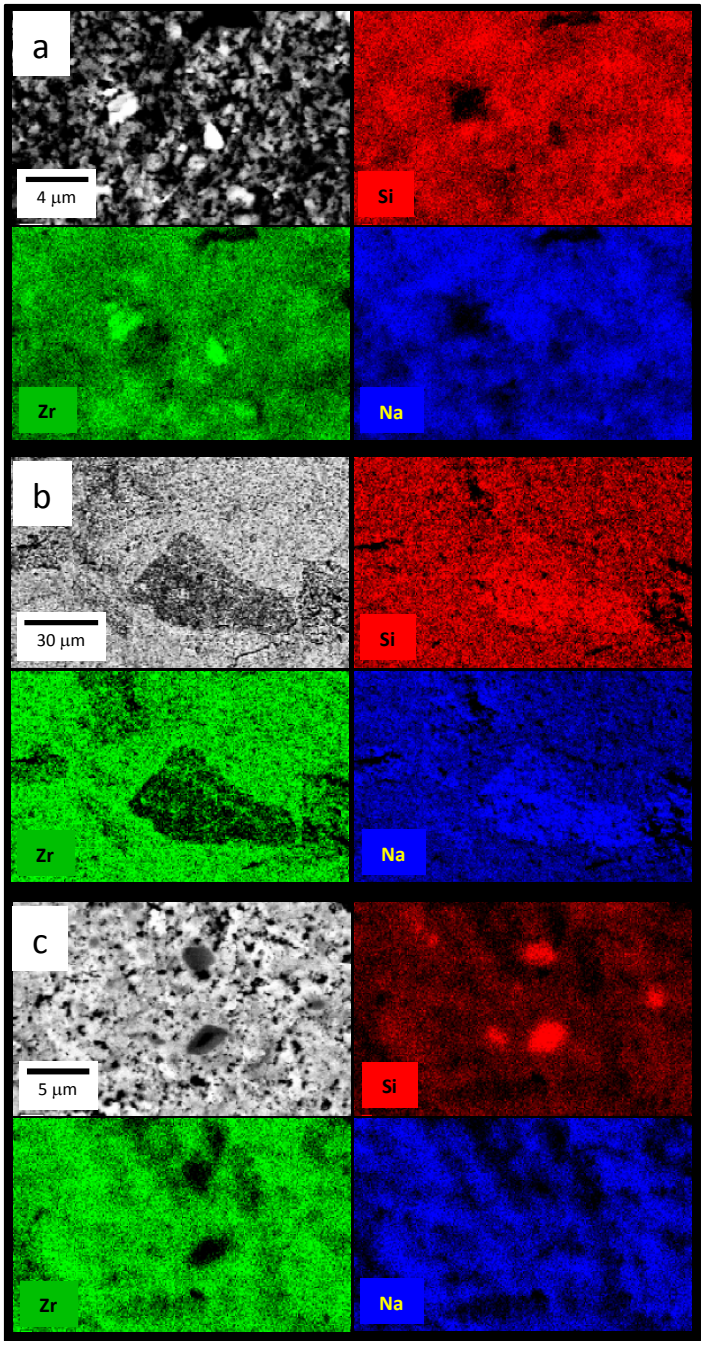

Figure 2. *Backscattered electron images and energy dispersive x-ray maps revealing the composition of contaminant phases in NaSICON ceramics. Maps are color coded according to elemental composition for Zr (green), Si (red) and Na (blue).*

Notably, none of these particular maps address the possibility of forming phosphate-based contaminants. Identification of the phosphorus in Zr-containing ceramics is complicated by the fact that the primary x-ray energies used to identify zirconium (Lα = 2.042 keV) overlap with the energy used to identify P (Kα = 2.015 keV). Any signal attributed to P will be confounded by signal from Zr. Fortunately, however, Zr also emits Kα x-rays with energy of 15.746 keV. By increasing the energy of incident electrons (above ~25keV), it is possible to detect the presence of Zr without confounding contribution from P x-rays. The panel of images displayed in Figure 3 illustrates how this approach can be used to identify the presence of sodium phosphate contaminants, similar to those seen in Figure 1h. The elemental maps reveal strong correlations between the contaminant inclusion and sodium, oxygen, and phosphorus/zirconium (at 2.042 keV). Meanwhile, there is a low correlation between the contaminant and silicon. Finally, there is a low correlation between the particle inclusion and the higher energy Zr peak. Comparing the higher energy Zr map with the lower energy P/Zr map allows us to infer that the included particle is rich in P, not Zr. Ultimately, these maps clearly show that the particle is a sodium phosphate contaminant.

The elemental maps in Figures 2 and 3 illustrate how EDXS can be used in concert with the BSE images of contaminants to provide crucial information about the chemical composition of these particles. It should be noted, however, that in most cases, this chemical information should be taken as *qualitative* data. Although EDXS on an SEM can be used to provide quantitative chemical information about a sample, there are specific requirements of sample preparation, configuration, and analysis (beyond the scope of this paper), which must be considered for EDXS data to be acceptable for quantitative analysis. Ultimately, coordination of data obtained using these approaches with more commonly reported analyses, such as XRD, can provide a much more informed and comprehensive picture of NaSICON's complex phase chemistry.

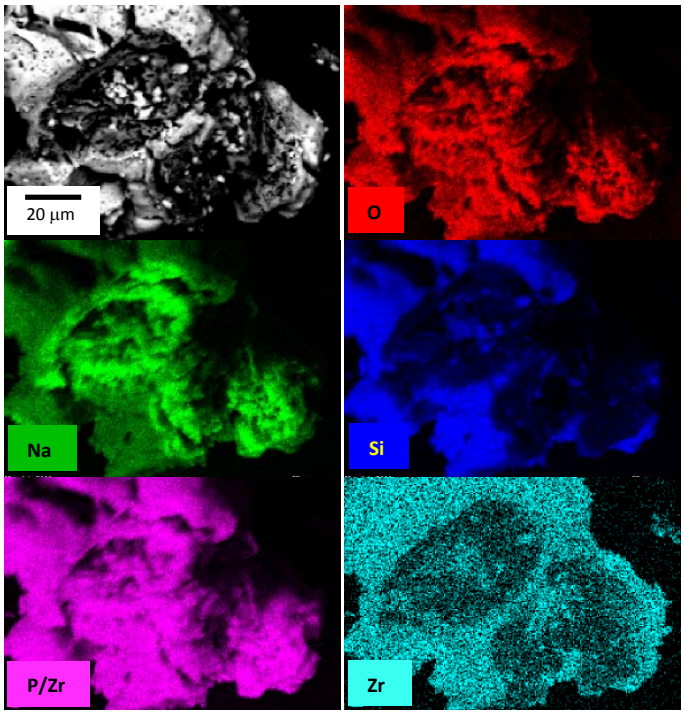

Figure 3. *Backscattered electron images and energy dispersive x-ray maps revealing the presence of sodium phosphates in NaSICON ceramics. Maps are color coded according to elemental composition for Na (green), O (red) and Si (blue), overlapping P/Zr (magenta) and high energy Zr (teal).*

CONCLUSIONS

NaSICON is a promising solid state electrolyte for emerging sodium-based energy storage systems, but as a material it is plagued by the formation of potentially deleterious secondary phases. Characterization of these secondary phases is crucial in determining their potential influences on NaSICON. Here, we show that the utilization of backscattered electron imaging and energy-dispersive x-ray spectroscopy can be used to provide a more complete picture of secondary phase morphology, distribution, and composition than is accessible using commonly applied methods such as x-ray diffraction and standard secondary electron imagining in an SEM. Incorporation of these relatively accessible capabilities into the characterization of materials such as NaSICON provides the opportunity to better understand the materials' challenges to developing these solid state ion conductors, and to design the improvements necessary to realize their potential utility in emerging battery technologies.

ACKNOWLEDGEMENTS

The authors gratefully acknowledge support from Energy Storage Program, managed by Dr. Imre Gyuk for the Department of Energy Office of Electricity Delivery and Energy Reliability. Sandia National Laboratories is a multi-program laboratory operated by Sandia Corporation, a wholly owned subsidiary of Lockheed Martin Company, for the US Department of Energy's National Nuclear Security Administration under contract DE-AC04-94AL85000.

REFERENCES

[1] R. O. Fuentes, F. M. Figueiredo, F. M. B. Marques, J. I. Franco, "Influence of microstructure on the electrical properties of NASICON materials", *Solid State Ionics*, **140**, 2001, pp. 173.

[2] J. B. Goodenough, H. Y. P. Hong, J. A. Kafalas, "Fast Na+-Ion Transport in Skeleton Structures", *Materials Research Bulletin*, **11**, 1976, pp. 203.

[3] H. Y. P. Hong, "Crystal-Structures and Crystal-Chemistry in System Na1+Xzr2sixp3-Xo12", *Materials Research Bulletin*, **11**, 1976, pp. 173.

[4] H.-B. Kang, N.-H. Cho, "Phase formation, sintering behavior, and electrical characteristics of NASICON compounds", *Journal of Materials Science*, **34**, 1999, pp. 5005.

[5] D. M. Zhu, Z. L. Xie, F. Luo, W. C. Zhou, "Electrical Properties of Hot Press Sintered NASICON Ceramics", *Key Engineering Materials*, **334-335**, 2007, pp. 149.

[6] A. Ahmad, T. A. Wheat, A. K. Kuriakose, J. D. Canaday, A. G. McDonald, "Dependance of the Properties of Nasicons on their Composition and Processing", *Solid State Ionics*, **24**, 1987, pp. 89.

[7] R. S. Gordon, G. R. Miller, B. J. McEntire, E. Beck, J. Rasmussen, "Fabrication and Characterization of NaSICON Electrolytes", *Solid State Ionics*, **3/4**, 1981, pp. 243.

[8] B. J. McEntire, R. A. Bartlett, G. R. Miller, R. S. Gordon, "Effect of Decomposition on the Densification and Properties of Nasicon Ceramic Electrolytes", *Journal of the American Ceramic Society*, **66**, 1983, pp. 738.

[9] U. Von Alpen, M. F. Bell, H. H. Hofer, "Compositional Dependence of the Electrochemical and Structural Parameters in the Nasicon System (Na1+Xsixzr2p3-Xo12)", *Solid State Ionics*, **3-4**, 1981, pp. 215.

[10] E. Traversa, L. Montanaro, H. Aono, Y. Sadaoka, "Synthesis of Nasicon with New Compositions for Electrochemical Carbon Dioxide Sensors", *Journal of Electroceramics*, **5**, 2000, pp. 261.

[11] K. Kreuer, U. Warhus, "NASICON Solid Electrolytes Part IV: Chemical Durability", *Materials Research Bulletin*, **21**, 1986, pp. 357.

[12] H. Schmid, L. De Jonghe, C. Cameron, "Chemical Stability of NASICON", *Solid State Ionics*, **6**, 1982, pp. 57.

[13] R. O. Fuentes, F. Figueiredo, F. M. B. Marques, J. I. Franco, "Reaction of NASICON with water", *Solid State Ionics*, **139**, 2001, pp. 309.

[14] D. Agrawal, J. Adair, "Low-Temperature Sol-Gel Synthesis of NaZr2P3O12", *Journal of the American Ceramic Society*, **73**, 1990, pp. 2153.

[15] J.-S. Lee, C.-M. Chang, Y. Lee, S.-H. Hong, "Spark Plasma Sintering (SPS) of NASICON Ceramics", *Journal of the American Ceramic Society*, **87**, 2004, pp. 305.

[16] O. Schaf, P. I. Llewellyn, P. Knauth, N. Kaabbuathong, M. L. diVona, S. Licoccia, E. Traversa, "Preparation and Electrical Properties of Dense Ceramics with NASICON Composition Sintered at Reduced Temperatures", *Journal of Electroceramics*, **13**, 2004, pp. 817.

[17] Y. Shimizu, Y. Azuma, S. Michishita, "Sol-gel synthesis of NASICON discs from aquous solution", *Journal of Materials Chemistry*, **7**, 1997, pp. 1487.

[18] A. Caneiro, P. Fabry, H. Khireddine, E. Siebert, "Performance Characteristics of Sodium Super Ionic Conductor Prepared by the Sol-Gel Route for Sodium Ion Sensors", *Analytical Chemistry*, **63**, 1991, pp. 2550.

[19] A. Essoumhi, C. Favotto, M. Mansori, P. Satre, "Synthesis and characterization of a NaSICON series with general formula Na2.8Zr2-ySi1.8-4yP1.2+4yO12 (0 <= y <= 0.45)", *Journal of Solid State Chemistry*, **177**, 2004, pp. 4475.

[20] P. Porkodi, V. Yegnaraman, P. Kamaraj, V. Kalyanavalli, D. Jeyakumar, "Synthesis of Nasicon-A Molecular Precursor-Based Approach", *Chemistry of Materials*, **20**, 2008, pp. 6410.